Available online at www.sciencedirect.com
ScienceDirect
Bioelectrochemistry 71 (2007) 99–106
Bioelectrochemistry
www.elsevier.com/locate/bioelechem

# pH-tunable equilibria in azocrown ethers with histidine moieties

Elżbieta Jabłonowska [a], Barbara Pałys [a], Ewa Wagner-Wysiecka, Marzena Jamrógiewicz, Jan F. Biernat [b], Renata Bilewicz [a,*]

[a] *Department of Chemistry, University of Warsaw, ul. Pasteura 1, 02093 Warsaw, Poland*
[b] *Department of Chemical Technology, Technical University of Gdańsk, ul. Narutowicza 11, 80952 Gdańsk, Poland*

Received 1 March 2006; received in revised form 7 September 2006; accepted 17 September 2006
Available online 26 September 2006

**Abstract**

The crown ethers with electro- and photoactive azo moieties containing substituents with mobile protons such as in the –COOH groups of histidine, show unique effect of pH switched on/off presence of the azo form. The differences observed for the electrochemical behavior of azocrown ethers with *N*-acetylhistidine and imidazole moieties reveal the interference of a chemical reduction pathway in strongly acidified solutions. This chemical reduction process leads to the formation of a hydrazine derivative which can be detected by its further electroreduction on the electrode surface. The involvement of chemical reduction is seen clearly in the presence of mobile protons of the –COOH group and mercury as the electrode substrate. The behaviour of the *N*-acetylhistidine azomacrocyle is similar to that of compounds known to exist in quinone–hydrazone tautomeric equilibria.


*Keywords:* Histidine derivative; Azocrown ether; Azocompound; Tautomeric equilibria; Voltammetry; Macrocycle

## 1. Introduction

Renewed interest in the azocompounds is connected with their applications in molecular switching, sensors and image storage devices with fast response time [1–8]. Azocompounds are used as photo- or redox active components of films deposited on solid substrates by the self-assembly or Langmuir–Blodgett methods [5–17]. Modification of the macrocycle or incorporation of various substituents may change in a controlled way the organization of the monolayers and tune the electrochemical and complexing properties of these systems [17–32]. The organization of the azocrown molecules in monolayers was found to depend e.g. on the geometry around the –N═N– moiety and on the presence of alkali metal cations in the subphase. Transition from *E*- to *Z*-isomer occurred under influence of UV-irradiation, while switching back from *Z*- to *E*-isomer could be induced by reduction or by addition of appropriate alkali metal cation forming a complex with the azocrown ligand. Changes in the monolayer electrochemical behavior are allowed to follow isomerization processes in the monolayer. In aqueous solutions, the diarylazo group is reduced to diarylhydrazine compound and in alkaline solutions *Z* and *E* isomers can be recognized by their different reduction potential [29–34].

Heterocyclic residues form integral part of biological systems [35–37]. The presence of histidine in active centers of enzymes is frequently decisive for their catalytic activity. The role of imidazole residue is often connected with hydrogen bond formation with the substrate or with residues forming peptide chains; imidazole also plays important role in transacylation processes. The macrocyclic derivative of histidine (Scheme 1 — compound **2**) described in the present paper, has a more acidic imidazole N–H residue due to the electron withdrawing properties of azo substituents, that simultaneously decreases electron density of the heterocyclic ring. Due to these properties the compound **2**-macrocyclic histidine derivative may compete with peptide histidine residues and may be considered as a useful tracer for peptides.

In the present paper, we describe the electrochemical behaviour of imidazole and *N*-acetylhistidine azocrown ethers [Scheme 1 — structures **1** and **2**] adsorbed on the electrode surface and explain the changes of the voltammograms observed upon changing pH of the solution.

* Corresponding author. Tel.: +48 22 8220211x345; fax: +48 22 8224889.
*E-mail address:* bilewicz@chem.uw.edu.pl (R. Bilewicz).

1567-5394/$ - see front matter © 2006 Elsevier B.V. All rights reserved.
doi:10.1016/j.bioelechem.2006.09.005

## 2. Experimental

### 2.1. Electrochemistry

All materials were of analytical grade. Distilled water was passed through a Milli-Q water purification system. The LiOH obtained from Merck, $HClO_4$ and citric acid from PPH POCH were used to prepare appropriate buffer solutions. The solutions were prepared daily. Voltammetric experiments were carried out in a three-electrode arrangement with saturated calomel reference electrode, platinum foil counter electrode and static mercury drop electrode, SMDE 1 (Laboratorni Pristroje) of 0.0015 $cm^2$, used in the hanging mode. The layers were adsorbed on mercury electrode from the appropriate buffer solution containing $5 \times 10^{-7}$ M azocompound. Eco Chemie Autolab system was used as the potentiostat.

### 2.2. Spectroscopy

Raman spectra were recorded using Jobin-Ivon T6400 spectrometer. The 514.5 nm line of an argon ion laser was used for excitation. The 514.5 nm line, falling into absorption band of both compounds, was chosen to take advantage of the resonance Raman enhancement, which in turn enables study of diluted solutions. The pH value of the studied solutions was controlled by the pH-meter.

$^1$H NMR spectra were recorded on Varian apparatus at 500 MHz; *J* are given in Hz. Mass spectra (EI) were taken on an AMD-604 spectrometer. UV–Vis spectra were recorded in water–DMF (4:1) on a Unicam UV-330 Spectrophotometer. 1 cm quartz cuvettes were used for spectroscopic measurements. IR spectra were taken on Mattson Genesis II FTIR apparatus.

### 2.3. Liquid chromatography

HPLC experiments were performed on a Merck-Hitachi apparatus equipped with UV–Vis 4250 Detector, L-6200A Intelligent pump and D-2500 Chromato-Integrator; HPLC column (150 mm × 4.4 mm), support Nucleodur 100–5 C18, flow rate of 1 mL/min, $\lambda$=420 nm and temperature of 25 °C.

### 2.4. Synthesis of compounds

The synthesis of unsubstituted imidazole crown ether **1** was described elsewhere [38]. The synthesis and structure of compound **4** was described in [39]. Preparative chromatography was performed on glass plates covered with silica gel (60 $F_{254}$ MERCK).

### 2.5. Preparation of the *N*-acetyl-L-histidine crown ether (sodium salt), **2**

First, two solutions were prepared:

Solution A: A suspension of bis-amine 5 (0.58 g; 2 mmol) [35,38,39], in 40 mL water was ice-cooled and acidified with conc. hydrochloric acid (1 mL). The clear solution was diazotized with sodium nitrite (0.28 g; 4.1 mmol) dissolved in 2 mL cold water to give bis-diazonium salt **6**.

Solution B. *N*-Acetyl-L-histidine 7 (0.2 g; 2 mmol) [40] and sodium hydroxide (0.2 g; 5 mmol) were dissolved in 40 mL water and ice-cooled.

The above cold solutions A and B were dropped with the same speed during 45 min into 600 mL (high dilution conditions) vigorously stirred ice-cooled water (pH about 11). The temperature of aqueous medium was kept at 10 °C. Stirring at 10° was continued for 1 h and then for 12 h at 25°. Afterwards the mixture was cooled to 0–5° and pH was adjusted to 5–6 with cold acetic acid (about 20 mL) to precipitate crude products.

The organic products were extracted using chloroform and acetic acid (50:1) mixture. After evaporation of the solvent, the residue was chromatographed on a column filled with silica gel 60 (63–200 μm; Fluka). The crown ether was eluted from the column using methylene chloride at the beginning, then with methylene chloride/methanol mixture 100:1, and finally methylene chloride/methanol 15:2 mixture to afford crown ether **2** (in

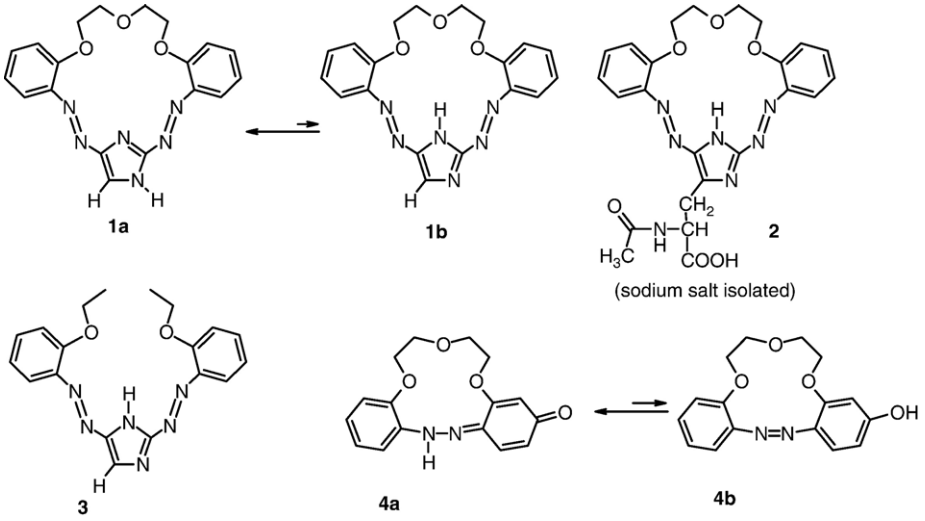


Scheme 1. Structures of studied imidazole (tautomers **1a** and **1b**) and *N*-acetylhistidine (**2**) azocrowns, a model of open bisazo imidazole derivative (**3**) and tautomeric forms of hydroxyazocrown ether (**4a** and **4b**).

form of sodium salt) (0.076 g, 15%), mp. 220–223 °C. TLC, $R_F$ 0.49 ($CH_2Cl_2$:MeOH 15:2); $R_F$ 0.34 ($CH_2Cl_2$:acetone 2:1). HPLC, eluent: methanol/water 1:4, retention time 1.37 min; eluent methanol/water 1:1, retention time 3.70 min. UV–Vis, $\lambda_{max}$ (MeCN)/nm 326, 430 and 505 ($\epsilon$/dm$^3$ mol$^{-1}$ cm$^{-1}$ 4870, 5600 and 7420); $\lambda_{max}$ (water–DMF 4:1)/nm 333, 385 and 506 ($\epsilon$/dm$^3$ mol$^{-1}$ cm$^{-1}$ 8900, 10 000 and 11 000). $\nu_{max}$ (nujol), 3337 (broad), 1588, 1301, 1243, 1160, 1111, 1061, 944, 756, 598. $\delta_H$ (500 MHz; DMSO; $Me_4Si$) 1.66 (3H, s, *CH*$_3$); 3.19–3.22 (2H, m, Ar*CH*$_2$); 3.80–4.00 (4H, m, *CH*$_2$O*CH*$_2$); 4.22–4.28 (1H, m, *CH*COO); 4.35–4.38 (4H, m, ArO*CH*$_2$); 7.01–7.07 (2H, m, Ar*H*); 7.23 (1H, d, $J_{1,3}$ 8.2, Ar*H*); 7.28–7.34 (2H, m, Ar*H*); 7.42 (1H, t, $J_{1,3}$ 7.4, Ar*H*); 7.45 (1H, d, $J_{1,3}$ 7.7, Ar*H*); 7.68 (1H, d, $J_{1,3}$ 7.8, Ar*H*). MS ESI: $[M + H]^+$ *m/z* 508.2; $C_{24}H_{25}N_7O_6$ requires 507.2; $[M + Na]^+$=530.2. HRMS ESI $[M + Na]^+$ *m/z* 530.1744; $C_{24}H_{25}N_7O_6$ requires 530.1758 (Scheme 2).

### 2.6. Preparation of the 2,4-bis(2-ethoxyphenylazo)imidazole, compound 3

First two solutions were prepared:

Solution C: *o*-Ethoxyaniline (0.26 mL, 2 mmol) was dissolved in 20 mL ice-cold water acidified with 1 mL conc. hydrochloric acid. To this solution sodium nitrite (0.14 g, 2.1 mmol) solution in 2 mL cold water was added.

Solution D: Imidazole (0.069 g, 1 mmol) and sodium hydroxide (0.2 g, 5 mmol) was dissolved in 150 mL water.

Both solutions were cooled (4 °C), and then solution C was added dropwise to a vigorously stirred solution D. The temperature was maintained below 10° for 1 h and later at room temperature for 12 h. Afterwards the reaction mixture was extracted three times with chloroform–acetic acid–toluene mixture (6:1:1). Product **3** was isolated using preparative TLC plates (0.022 g, 6%). Mp 137–142°. $R_F$ 0.9 (methylene chloride–acetone 1:1) and 0.5 (methylene chloride–acetone 10:1). $\lambda_{max}$ (water–DMF 4:1)/nm 355 ($\epsilon$/dm$^3$ mol$^{-1}$ cm$^{-1}$ 5000). $\nu_{max}$ (film) 3118, 2982, 2826, 1590, 1487, 1471, 1397, 1308, 1281, 1237, 1159, 1116, 1040, 923, 754. $\delta_H$ ($CDCl_3$; 500 MHz; $Me_4Si$) 1.56 (6H, t, $J_{1,3}$ 6.8, *CH*$_3$); 4.24 (4H, q, $J_{1,3}$ 6.8, ArO*CH*$_2$); 7.02 (2H, t, $J_{1,3}$ 7.8, Ar*H*); 7.09 (2H, t, $J_{1,3}$ 6.3, Ar*H*); 7.43 (1H, t, $J_{1,3}$ 7.3, Ar*H*); 7.49 (1H, t, $J_{1,3}$ 7.3, Ar*H*); 7.78 (1H, d, $J_{1,3}$ 7.8, Ar*H*); 7.94 (1H, d, $J_{1,3}$ 8.3, Ar*H*); 8.08 (1H, s, Ar*H*); –*NH* (out of sight); $\delta_H$ (DMSO; 500 MHz; $Me_4Si$) 1.41–1.46 (6H, m, O–$CH_2$*CH*$_3$); 4.23–4.32 (4H, m, O–*CH*$_2$$CH_3$); 7.01 (1H, t, $J_{1,3}$ 7.5, Ar*H*); 7.07 (1H, t, $J_{1,3}$ 7.5, Ar*H*); 7.24 (1H, d, $J_{1,3}$ 8.2, Ar*H*); 7.30 (1H, d, $J_{1,3}$ 8.2, Ar*H*); 7.46 (1H, t, $J_{1,3}$ 6.8, Ar*H*); 7.51–7.58 (3H, m, Ar*H*); 8.01 (1H, s, Ar*H*); 13.51 (1H, s, N*H*).

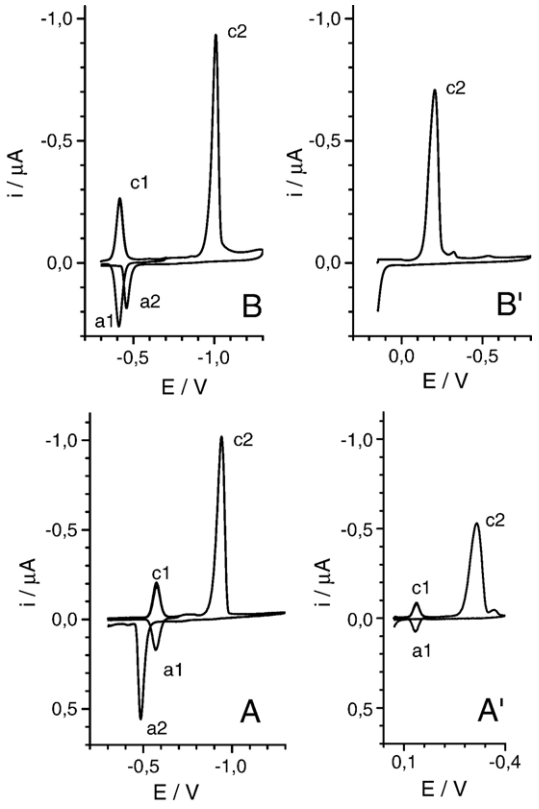


Fig. 1. Voltammograms for $5 \cdot 10^{-7}$ M compound **1** (A) and **2** (B) recorded in 0.1 M citric acid–LiOH buffer solution, $\nu$=0.1 V/s, $t_{adsorption}$=2 min. at pH 12.0 (A, B) and pH 3 (A', B').

MS (EI): $M^+$=364; $C_{19}H_{20}N_6O_2$ requires 364. HRMS (EI): $M^+$=364.16444; calculated 364.16477.

### 2.7. Spectral properties of azocrown ether 1

$\lambda_{max}$ (water–DMF 4:1)/nm 381, 420–500 (broad) ($\epsilon$/dm$^3$ mol$^{-1}$cm$^{-1}$ 3580, ~ 2900).

### 2.8. Spectral properties of compound (4)

$\lambda_{max}$ (water–DMF 4:1)/nm 459 ($\epsilon$/dm$^3$ mol$^{-1}$cm$^{-1}$ 4400).

## 3. Results and discussion

### 3.1. Electrochemistry

The compounds **1** and **2** (Scheme 1) were adsorbed for 2 min on the electrode surface from a diluted $5 \cdot 10^{-7}$M solution of

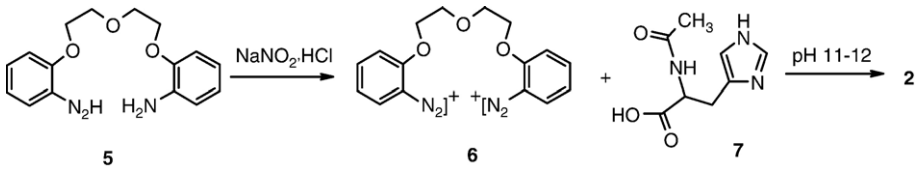


Scheme 2. Synthesis route leading to macrocyclic *N*-acetylhistidine derivative.

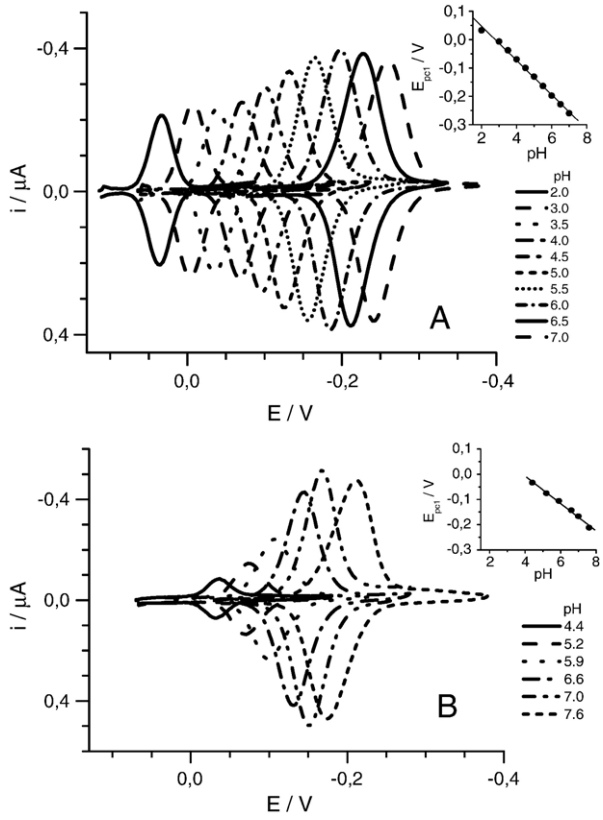


Fig. 2. A. Voltammograms for $5 \cdot 10^{-7}$ M compound **1** recorded in 0.1 M citric acid–LiOH buffer solution of decreasing pH from 7.0 to 2.0, $v$=0.1 V/s, $t_{adsorption}$=2 min. B. Voltammograms for $5 \cdot 10^{-7}$ M compound **2** recorded in 0.1 M citric acid–LiOH buffer solution of decreasing pH from 7.6 to 4.4, $v$=0.1 V/s, $t_{adsorption}$=2 min. Inset — $E_{pc1}$ vs. pH plot.

azocrown. The voltammograms recorded in alkaline solution, pH 12, for the imidazole derivative (compound **1**) are shown in Fig. 1A and for the histidine one (compound **2**) — in Fig. 1B. At pH 12, the electrode processes of both compounds are similar. Two reduction peaks correspond to a 2e reduction to disubstituted hydrazine form (peak c1) and next to the diamine (peak c2).

In acidified solutions of compound **1** the peak c1 (Fig. 1A) is shifted towards more positive potentials and smaller than in alkaline media (Fig. 4A) while for compound **2** it disappears completely (Fig 1B'). Under these conditions (pH 2) mercury is oxidized at + 0.2 V.

For the imidazole azocrown, below pH 4 the charge of the peak c1 is approximately constant (Fig. 2A).

The slope of the cathodic peak c1 potential vs. pH plot is 60 mV in the range 2.5 to 11.5 indicating that 1 proton is consumed in the rate determining step. The peak c2 is shifted by 74 mV with a unit increase in pH.

Above pH 6 the charge of the peak $c_1$ is however twice that of the peak in acidified solutions. This means that above this pH all azogroups are reduced while in acidic solution only part of them is available for electroreduction on the electrode surface.

In case of the histidine derivative (compound **2**), the situation is different — no c1 peak is found below pH 4.0 (Fig. 2B). Above this pH, the charge increases and attains approximately constant value in alkaline solution. Thus below pH 4.0 no azo moiety is present on the electrode for the histidine derivative. As shown in Fig 1B', the voltammogram recorded in solution of pH 3 contains only one signal — c2, corresponding to the respective hydrazine form reduction. Thus acidified solutions promote chemical reduction of the azo bond to the hydrazine form and this process is facilitated by the presence of substituents containing mobile protons in the adsorbed molecule. In contrary to peak c1, the peak c2 has almost constant charge over the whole pH range for all derivatives studied. Its width is pH and

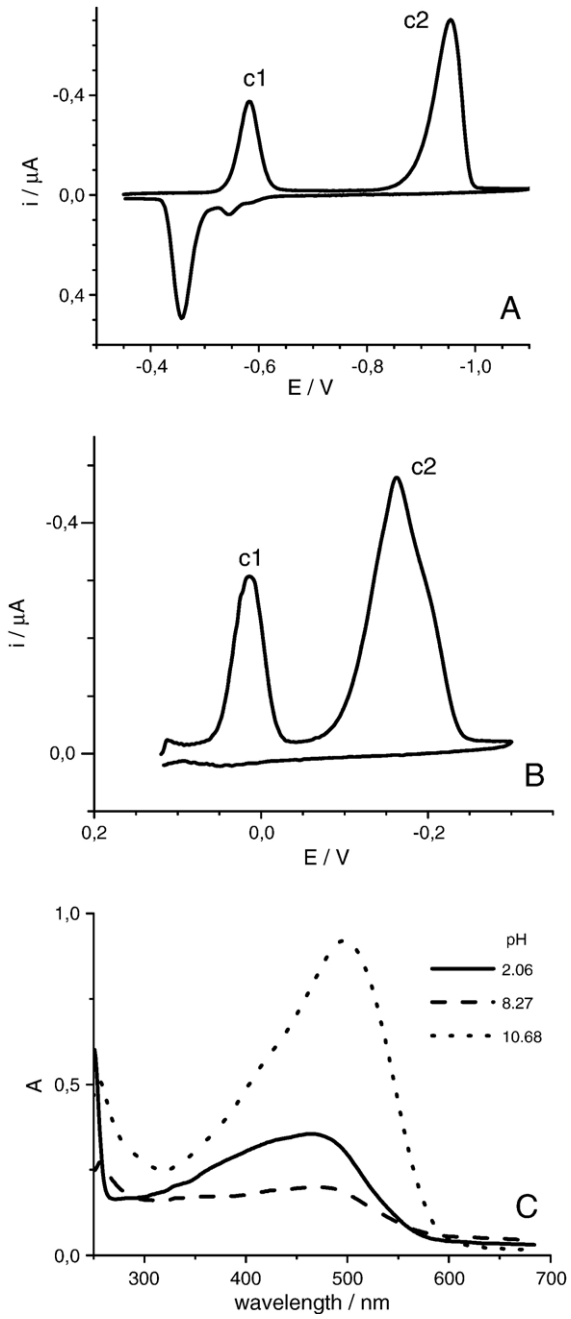


Fig. 3. Voltammograms for $5 \cdot 10^{-7}$ M compound **3** recorded in 0.1 M citric acid–LiOH buffer solution, $v$=0.1 V/s, $t_{adsorption}$=2 min. at pH 12.0 (A) and pH 3 (B). (C) UV–Vis spectrum of compound **3** in water–DMF (4:1) at different pH (lithium citrate buffer).

supporting electrolyte dependent. In acidified perchlorates it is lower and wider indicating some repulsion in the layer. The influence of pH on the magnitude of the c1 peak is much smaller for the open compound **3** as shown in Fig. 3 and both c1 and c2 peaks are present in the whole pH range.

Protonation of compound **3** in the solution (Fig. 3C) proceeds easier as compared to compound **1**. Again dissociation of imidazole proton is seen at higher pH values.

Several cases of tautomerism have been reported for azophenol compounds. We described such azophenol⇌quinone monohydrazone tautomeric equilibria for macrocyclic compounds in a recent review [40] and in [35] for compound **4**. Compound **4** also undergoes adsorption on Hg but peak c1 is hardly seen in alkaline solutions (Fig. 4A) and fully disappears at low pH (Fig. 4B).

This indicates that equilibrium for the compounds **4a⇌4b** (Scheme 1) is so strongly shifted to the left side that practically no azo form is present at the electrode surface.

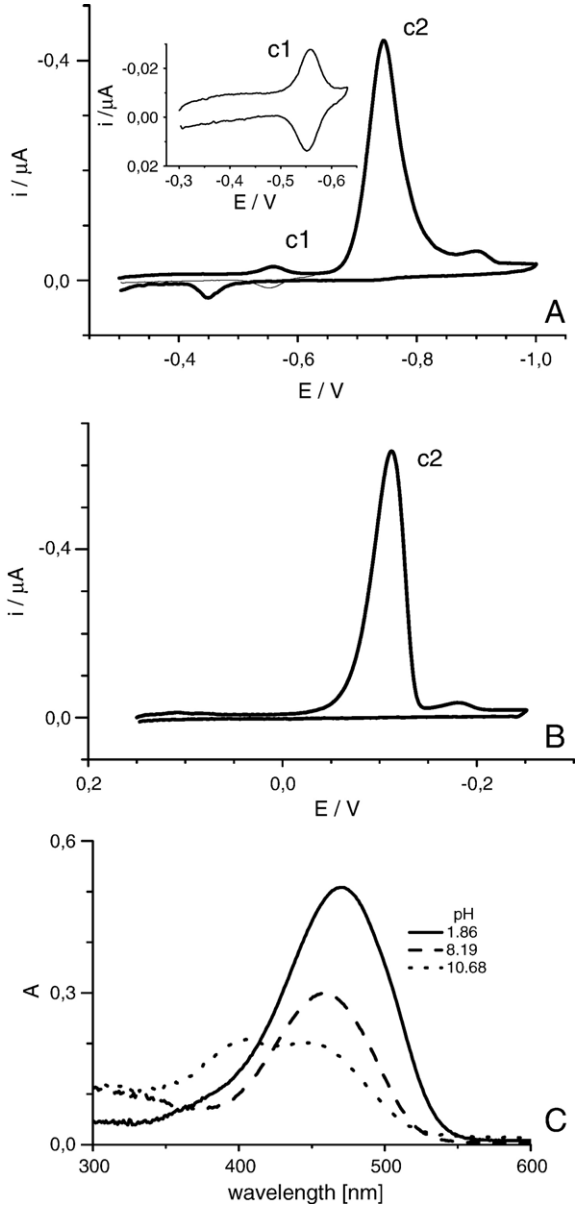


Fig. 4. Voltammograms for $5 \cdot 10^{-7}$ M compound **4** recorded in 0.1 M citric acid–LiOH buffer solution, $v$=0.1 V/s, $t_{adsorption}$=2 min. at pH 12.0 (A) and pH 3 (B). (C) UV–Vis spectra in water–DMF (4:1) solution at different pH (lithium citrate buffer).

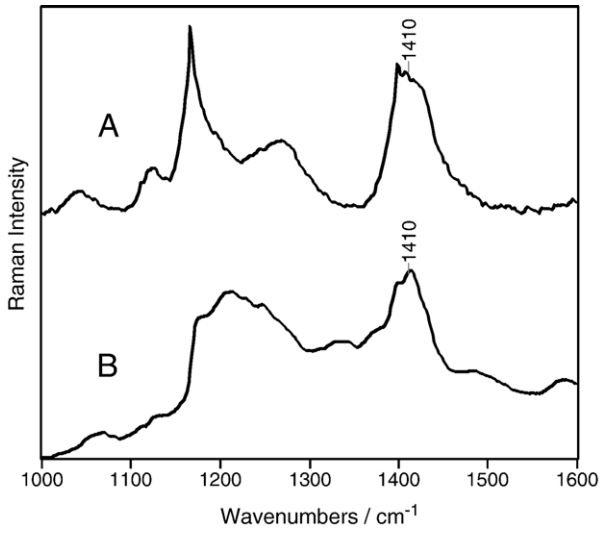


Fig. 5. Raman spectra of: A) imidazole (compound **1**) and B) histidine derivative (compound **2**) of azocrown recorded in the basic solution, pH 12. Excitation line 514.5 nm.

### *3.2. Raman spectra of the imidazole and histidine derivatives of azocrowns in aqueous solutions*

In aqueous alkaline solution of pH 12, the N═N bands for the imidazole and *N*-acetylhistidine azocrown molecules are similar and appear at 1410 $cm^{-1}$. Fig. 5 presents the Raman spectra of the compounds **1** and **2** [Scheme 1] studied.

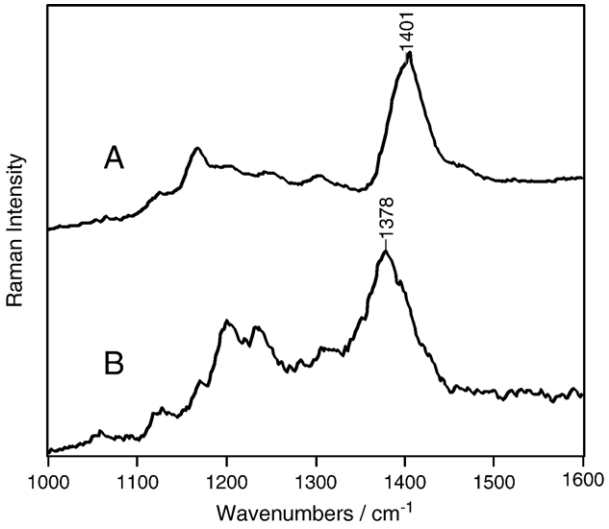


Fig. 6. Raman spectra of: A) imidazole (compound **1**) and B) histidine derivative (compound **2**) of azocrown recorded in the acidic solution, pH 3. Excitation line 514.5 nm.

In acidified solution, pH 3 (Fig. 6) the N═N bands for both compounds appear at lower wavenumbers due to possible protonation of azo groups.

Interestingly, for the imidazole derivative (compound **1**) the band appears at 1401 $cm^{-1}$ while for the histidine derivative (compound **2**) it occurs at distinctly lower (1378 $cm^{-1}$) wavelength, indicating larger charge delocalization for histidine derivative in comparison to the imidazole containing compound. Furthermore, spectra of the imidazole and acetylhistidine substituted compounds reveal significant differences in relative band intensities in the 1100–1300 $cm^{-1}$ range, comprising imidazole ring deformation modes. Such differences may also originate from differences in charge distribution, which in turn influence the resonance Raman intensities. These results may point to intramolecular hydrogen bonding between the carboxylic group and the azo group.

### 3.3. NMR experiments in nonaqueous solutions

The $^1$H NMR (*d*-DMSO; 500 MHz) NOE experiments show that the imidazole proton –NH (δ 10.56 ppm) is close to the imidazole –CH indicating that structure 1a dominates [Scheme 1].

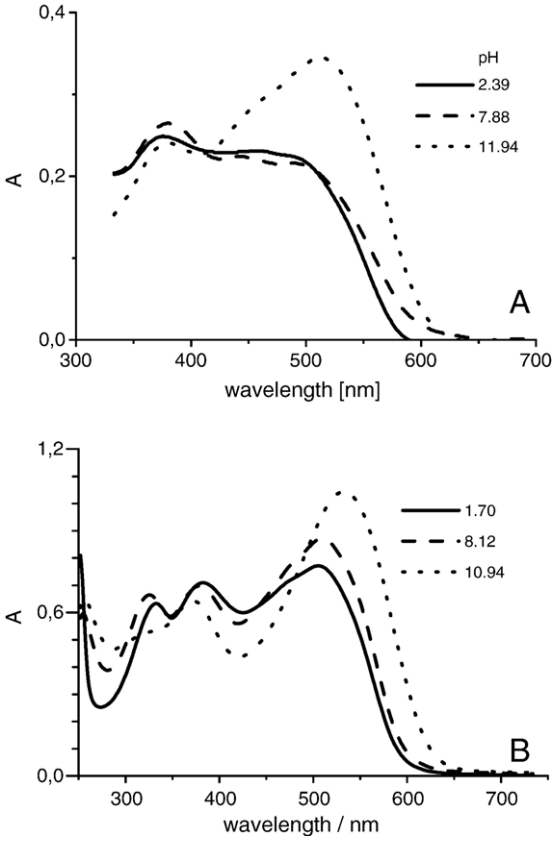


Fig. 7. A. Spectra of compound **1** dissolved in water: DMF (4:1) mixture. Crown ether concentration $7.4 \cdot 10^{-5}$ mol·$dm^{-3}$. The spectra were registered at pH 2.39 (citric acid, 1 mol·$dm^{-3}$), pH 7.88 (lithium citrate 1 mol·$dm^{-3}$) and at pH 11.94 (lithium citrate adjusted with LiOH). B. Spectra of compound **2** dissolved in water:DMF (4:1) mixture. Crown ether concentration $7.1 \cdot 10^{-5}$ mol·$dm^{-3}$. The spectra were registered at pH 1.70 (citric acid 1 mol·$dm^{-3}$), pH 8.12 (lithium citrate 1 mol·$dm^{-3}$) and at pH 10.94 (lithium citrate adjusted with LiOH).

Following 100-fold magnification of the spectrum also a weak signal from –NH is seen at ca. 14 ppm, indicating the contribution of form 1b. The equilibrium of the prototropic tautomerism is, however, strongly shifted towards the formation of tautomer 1a with an "outer" location of the –NH group. In *N*-acetylhistidine crown ether due to lack of NOE effect the structure corresponds to formula 2.

### 3.4. UV–Vis experiments in water–DMF solutions

UV–Vis spectra of the compounds **1**–**4** were recorded in water–DMF (4:1) solutions of different pH (Figs. 3C, 4C and 7).

The absorption of compound **1** is not changed with changes fromacidic to slightly basic conditions. However, at pH ~ 12 the band at around 500 nm increases with simultaneous batochromic shift indicating imidazole NH proton abstraction. This is in agreement with $pK_a$ value (~10) assessed by analogy to phenylazoimidazole derivatives [41]. In the spectra of *N*-acetylhistidine azocrown ether **2** (Fig. 7B) the absorption bands are stronger and shifted to longer wavelengths; the release of one proton occurs under slightly alkaline conditions (pH 8) and the imidazole proton dissociation is visible at pH 11. At low pH protonation of the quinone–hydrazone form is indicated by increase of spectral band at 470 nm. At high pH the presence of azo group is indicated by distinct band at around 400 nm.

$^1$H and $^{13}$C NMR, and UV–Vis spectra of compound **4** in methanol, chloroform and in acetonitrile confirm existence of only form **4a** (Scheme 1). For acetonitrile solution $\lambda_{max}$ = 434 nm, $\epsilon_{max} = 2.31\ 10^4$ [38]. This confirms that equilibrium for the compounds **4a 4b** (Scheme 1) is strongly shifted to the left side.

## 4. Conclusions

The system of voltammetric peaks c1/a1 corresponding to reaction:

$$-N = N- + 2e + 2H^+ = [-NH-NH-]$$

was found to diminish under certain conditions for azocrown ethers containing substituents with mobile protons. For *N*-acetylhistidine azomacrocycle **2** as well as for the azophenol derivative **4**, the first step of reduction disappears below pH 4.0 showing that no azo moiety is present at the electrode, while the second step remains unaffected. This behavior shows that the azo form of these compounds undergoes transformation to the hydrazine form not by means of an electrode process but following a chemical pathway. Under these conditions mercury may play the role of reducing agent in the chemical reaction pathway. The two pathways lead to the formation of same hydrazine derivative which remains at the electrode surface and undergoes further reduction according to equation:

$$[-NH-NH-] + 2e + 2H^+ = [-NH_2\ NH_2-]$$

Protonation of azo residue(s) or their involvement in hydrogen bonding was confirmed by the Raman and UV–Vis spectra in solution. Above pH 4, when the –COOH group of histidine

undergoes dissociation both steps of the electroreduction are observed indicating that the compound is present on the electrode surface in its original electrochemically reducible azo form. The proton transfer reaction described here leading to the disappearance of the first step of the electrode process on mercury electrode is unique in that it is connected with substituents possessing labile protons. This has to be kept in mind when thin films of molecules with redox- and photoactive azo moieties are used in acidified solutions.

## Acknowledgement

This work was financially supported by Ministry of Scientific Research and Information Technology, Project No. PBZ 18-KBN-098/T09/2003, grant No 3 T09A 151 27 and from the Gdańsk University of Technology (DS grant No. 014668/003). We appreciate Dr. E. Luboch for the kind delivery of compound **4** and MSc. K. Sadowska for the assistance.

## References

[1] K. Kano, Y. Tanaka, T. Ogawa, M. Shimomura, Y. Okahata, T. Kunitake, Photoresponsive membranes. Regulation of membrane properties by photoresponsible *cis–trans* isomerization of azobenzenes, Chem. Lett. (1980) 421–424.
[2] S. Shinkai, O. Manabe, Photocontrol of ion extraction and ion-transport by photofunctional crown ethers, Top. Curr. Chem. 121 (1984) 67–104.
[3] Y. Einaga, Z.-Z. Gu, S. Hayami, A. Fujishima, O. Sato, Reversible photoinduced switching of magnetic properties at room temperature of iron oxide particles in self-assembled films containing azobenzene, Thin Solid Films 374 (2000) 109–113.
[4] T. Ikeda, O. Tstsumi, Optical switching and image storage by means of azobenzene liquid-crystal films, Science 268 (1995) 1873–1875.
[5] T. Nagele, R. Hoche, W. Zinth, J. Wachtveitl, Femtosecond photoisomerization of *cis*-azobenzene, Chem. Phys. Lett. 272 (1997) 489–495.
[6] R.A. Moss, W. Jiang, Thermal modulation of photoisomerization in double-azobenzene-chain liposomes, Langmuir 13 (1997) 4498–4501.
[7] Y. Ren, Y. Tian, R. Sun, S. Xi, Y. Zhao, X. Huang, Structure and photoisomerization of the Z-type Langmuir–Blodgett films of a new series of azo-containing chiral copolymers, Langmuir 13 (1997) 5120–5124.
[8] R. Wang, T. Iyoda, D.A. Tryk, K. Hashimoto, A. Fujishima, Electrochemical modulation of molecular conversion in an azobenzene-terminated self-assembled monolayer film: an in situ UV–visible and infrared study, Langmuir 13 (1997) 4644–4651.
[9] Z.F. Liu, C.X. Zhao, M. Tang, S.M. Cai, Electrochemistry of *cis*-azobenzene chromophore in coulombically linked self-assembled monolayer-Langmuir–Blodgett composite monolayers, J. Phys. Chem. 100 (1996) 17337–17344.
[10] J. Zhang, J. Zhao, H.L. Zhang, H.L. Li, Z.F. Liu, Structural evaluation of azobenzene-functionalized self-assembled monolayers on gold by reflectance FTIR spectroscopy, Chem. Phys. Lett. 271 (1997) 90–94.
[11] B.R. Herr, C.A. Mirkin, Self-assembled monolayers of ferrocenylazobenzenes: monolayer structure vs response, J. Am. Chem. Soc. 116 (1994) 1157–1158.
[12] W.B. Caldwell, K.M. Chen, B.R. Herr, C.A. Mirkin, J.C. Hulteen, R.P.V. Duyne, Self-assembled monolayers of ferrocenylazobenzenes on Au(111)/mica films: surface-enhanced Raman scattering response vs surface morphology, Langmuir 10 (1994) 4109–4115.
[13] W.B. Caldwell, D.J. Campbell, K.M. Chen, B.R. Herr, C.A. Mirkin, A. Malik, M.K. Durbin, P. Dutta, K.G. Huang, A highly ordered self-assembled monolayer film of an azobenzenealkanethiol on Au(111): electrochemical properties and structural characterization by synchrotron in-plane X-ray diffraction, atomic force microscopy, and surface-enhanced Raman spectroscopy, J. Am. Chem. Soc. 117 (1995) 6071–6082.
[14] Z.F. Liu, K. Hashimoto, A. Fujishima, Photoelectrochemical information storage using an azobenzene derivative, Nature 347 (1990) 658–660.
[15] Z.F. Liu, K. Hashimoto, A. Fujishima, Kinetic studies on the thermal *cis–trans* isomerization of an azo compound in the assembled monolayer film, J. Phys. Chem. 96 (1992) 1875–1880.
[16] Z.F. Liu, B.H. Loo, K. Hashimoto, A. Fujishima, A novel photoelectrochemical hybrid "one-way" process observed in the azobenzene system, J. Electroanal. Chem. 297 (1991) 133–144.
[17] R. Bilewicz, Molecular design of electrode surface for electoanalytical chemistry, Ann. Chim. 87 (1997) 53–66.
[18] J.F. Biernat, E. Luboch, A. Cygan, Y.A. Simonov, A.A. Dvorkin, E. Muszalska, R. Bilewicz, Synthesis, x-ray structure and electochemical properties of a new crown ether with a cis azo unit in the macrocycle, Tetrahedron 48 (1992) 4399–4406.
[19] E. Luboch, J.F. Biernat, E. Muszalska, R. Bilewicz, 13-membered crown ethers with azo or azoxy unit in the macrocycle — synthesis, membrane electrodes, voltammetry and Langmuir monolayers, Supramol. Chem. 5 (1995) 201–210.
[20] I. Zawisza, E. Luboch, J.F. Biernat, R. Bilewicz, Properties of *Z* and *E* isomers of azocrown ethers in monolayer assemblies at the air–water interface, Thin Solid Films 348 (1999) 173–179.
[21] H. Huesmann, J. Maack, D. Möbius, Molecular cis/trans isomerization of an azobenzene containing 13-azo-phane-3 in monolayer, J.F. Biernat, Sens. Actuators B 29 (1995) 148–153.
[22] E. Muszalska, R. Bilewicz, Adsorptive stripping analysis and monolayer properties of crown ethers with an azo unit in the macrocycle, Analyst 119 (1994) 1235–1238.
[23] L.M. Goldenberg, J.F. Biernat, M.C. Petty, Electro- and photochemistry of 13-membered azocrowns in solution and as Langmuir–Blodgett films, Langmuir 14 (1998) 1236–1241.
[24] I. Zawisza, R. Bilewicz, E. Luboch, J.F. Biernat, Langmuir–Blodgett films of azocrown ethers on electrodes — voltammetric recognition of isomers, J. Electroanal. Chem. 471 (1999) 156–166.
[25] I. Zawisza, R. Bilewicz, E. Luboch, J.F. Biernat, Voltammmetric recognition of cis (*Z*) and trans *(E*) isomers of azobenzene and azocrown ethers, Supramol. Chem. 9 (1998) 277–287.
[26] K. Janus, J. Sworakowski, A. Olszowski, A. Lewanowicz, J. Lipiński, E. Luboch, J.F. Biernat, Kinetics of a photochromic reaction in a dibenzoazo crown ether in solution and in polymer matrices, Adv. Mater. Opt. Electron. 9 (1999) 181–187.
[27] I. Zawisza, R. Bilewicz, E. Luboch, J.F. Biernat, Effect of binding cations on the electorchemical behavior of azocrown ethers in Langmuir–Blodgett films, J. Chem. Soc., Dalton Trans. 4 (2000) 499–503.
[28] I. Zawisza, R. Bilewicz, M.R. Moncelli, R. Guidelli, Electrochemistry of Langmuir–Blodgett and self-organized monolayers of an azocrown ether, both pure and mixed with a phospholipid, J. Electroanal. Chem. 509 (2001) 31–41.
[29] E. Luboch, J.F. Biernat, Y.A. Simonov, A.A. Dvorkin, Synthesis and electrode properties of 16-membered azo- and azoxycrown ethers. Structure of tribenzo-16-azocrown-6, Tetrahedron 54 (1998) 4977–4990.
[30] J.F. Biernat, E. Luboch, A. Skwierawska, R. Bilewicz, E. Muszalska, Azocrown ethers as ion sensing compounds, Biocyb. Biomed. Eng. 16 (1996) 125–135.
[31] A. Skwierawska, H.D. Inerowicz, J.F. Biernat, Chromogenic proton-dissociable azocrown ether reagents for lithium ions, Tetrahedron Lett. 39 (1998) 3057–3060.
[32] E. Wagner-Wysiecka, A. Skwierawska, V.Ch. Kravtsov, J.F. Biernat, New class of chromogenic proton-dissociable azocrown reagents for alkali metal ions, J. Supramol. Chem. 1 (2) (2001) 77–85.
[33] E. Luboch, R. Bilewicz, M. Kowalczyk, E. Wagner-Wysiecka, J.F. Biernat, Azomacrocyclic compounds, in: G.W. Gokel (Ed.), Advances in Supramolecular Chemistry, vol. 9, Cerberus Press Inc., 2003, pp. 73–163.
[34] E. Luboch, Z. Poleska-Muchlado, M. Jamrógiewicz, J.F. Biernat, in: K. Gloe (Ed.), Macrocyclic Chemistry, Current Trends and Future Perspectives, Springer, 2005, pp. 203–218, Chapter 13. Cyclodextrin Combinations with Azocompounds.
[35] Y.A. Ovchinnikov, V.T. Ivanov, A.M. Shkrob, Membrane Active Complexones, Elsevier, New York, 1974.

[36] B.C. Pressman, Biological applications of ionophores, Ann. Rev. Biochem. 45 (1976) 501–530.
[37] R.W. Hay, Bio-Inorganic Chemistry, Ellis Horwood, Chichester, 1984.
[38] E. Wagner-Wysiecka, E. Luboch, M. Kowalczyk, J.F. Biernat, Chromogenic macrocyclic derivatives of azoles — synthesis and properties, Tetrahedron 59 (2003) 4415–4420.
[39] E. Luboch, E. Wagner-Wysiecka, J.F. Biernat, Chromogenic azocrown ethers with peripheral alkyl, alkoxy, hydroxy or dimethylamino group, J. Supramol. Chem. 2 (2003) 279–291.
[40] R.M. Herbst, D. Shemin, Acetylglycine, organic syntheses, Coll. II (1947) 11–12.
[41] D. Maciejewska, L. Skulski, UV–Vis solution spectra of 2-arylazoimidazoles and of their 1-*N*-methyl derivatives as compared with those of the respective azobenzenes. Exemplary application of empirical methods of spectral characterization of some complex aryazo substituted groups, Pol. J. Chem. 57 (1983) 971–984.